

Three criteria for particle acceleration in collisionless shocks

Antoine Bret^{1,2} and Asaf Pe'er³

Research Article

Cite this article: Bret A, Pe'er A (2018). Three criteria for particle acceleration in collisionless shocks. *Laser and Particle Beams* **36**, 458–464. <https://doi.org/10.1017/S0263034618000472>

Received: 23 July 2018
Revised: 7 November 2018
Accepted: 11 November 2018

Key words:

collisionless shocks; particle acceleration

Author for correspondence:

Antoine Bret, ETSI Industriales, Universidad de Castilla-La Mancha, 13071 Ciudad Real, Spain and Instituto de Investigaciones Energéticas y Aplicaciones Industriales, Campus Universitario de Ciudad Real, 13071 Ciudad Real, Spain, E-mail: antoineclaude.bret@uclm.es

¹ETSI Industriales, Universidad de Castilla-La Mancha, 13071 Ciudad Real, Spain; ²Instituto de Investigaciones Energéticas y Aplicaciones Industriales, Campus Universitario de Ciudad Real, 13071 Ciudad Real, Spain and ³Department of Physics, Bar-Ilan University, Ramat-Gan, 52900, Israel

Abstract

Collisionless shocks have been the subject on many studies in recent years, due to their ability to accelerate particles. In order to do so, a shock must fulfill three criteria. First, it must be strong enough to accelerate particles efficiently. Second, both the upstream and the downstream must be collisionless. Third, the shock front must be surrounded by electromagnetic turbulence capable of scattering particles back and forth. We here consider the encounter of two identical plasma shells with initial density, temperature, and velocity n_0 , T_0 , v_0 , respectively. We translate the three criteria to the corresponding requirements on these parameters. A non-trivial map of the allowed region for particle acceleration emerges in the (n_0, T_0, v_0) phase space, especially at low velocities or high densities. We first assess the case of pair plasma shells, before we turn to electrons/protons.

Introduction

In a fluid, energy dissipation at the front of a shockwave is provided by binary collisions. As a consequence, the width of the front is a few mean free path thick (Zel'dovich and Raizer, 2002). Yet, in a plasma, a shockwave can propagate with a front far smaller than the mean free path. For example, the front of the bow shock of the earth magnetosphere in the solar wind is about 100 km thick, while the mean free path at the same location is of the order of the Sun Earth distance (Bale *et al.*, 2003; Schwartz *et al.*, 2011).

Such shocks have been dubbed “collisionless shocks” and are exclusively mediated by collective plasma effects (Sagdeev, 1966). An interesting consequence of the absence of binary collisions is that particles can gather energy without sharing it with the others. Indeed, collisionless shock have been found excellent particle accelerators, which explains in great part the large amount of work that has been dedicated to them in the last decades (Blandford and Eichler, 1987; Kirk and Duffy, 1999; Dieckmann, 2005; Niemiec *et al.*, 2012; Marcowith *et al.*, 2016; Ruyer *et al.*, 2017; Yuan *et al.*, 2017).

In collisionless shocks, particles are accelerated when going back and forth around the shock front. Because of the difference of bulk velocity on each side of the front, energy is gained at each crossing until the particles escape upstream or downstream. We thus find three implicit assumptions are made at this stage:

- (1) The shock must be strong enough. A collisionless shock with a density compression ratio r accelerates particles with a power-law distribution of index $q \propto (r - 1)^{-1}$ (Blandford and Ostriker, 1978). Therefore, a weak shock with $r = 1 + \epsilon$ will not be an efficient particle accelerator.
- (2) Particles must be able to travel back and forth around the front. This implies that both the upstream and the downstream are collisionless, for if any is collisional, particles will be captured as soon as they enter it, no longer being able to travel across the front.
- (3) In order to scatter particles, the vicinity of the front must be electromagnetically turbulent. This turbulence arises in the downstream from the growth of beam–plasma instabilities during the shock formation (Bret *et al.*, 2013b, 2014). Once the shock is formed, the upstream turbulence is prompted by the unstable interaction of the upstream plasma with particles reflected at the front, and/or by accelerated particles escaping ahead of the front (Nakar *et al.*, 2011; Lemoine *et al.*, 2014). At any rate, the shock formation must have been mediated by plasma instabilities instead of binary collisions between particles of the two shells.

This article will explore these three requirements. We will first consider a system consisting in two colliding identical pair plasma shells. Their initial densities (in the laboratory frame), temperatures (comoving), velocities and Lorentz factor are n_0 , T_0 , $\pm v_0$ and

$\gamma_0 = (1 - v_0^2/c^2)^{-1/2}$. At each step, we will study how the three aforementioned criteria translate to the parameters (n_0, T_0, γ_0) .

As we will see, the strong shock requirement constrains the range of allowed temperatures. As a result, criteria 2 and 3 can be assessed assuming $T_0 = 0$. Only criterion 1 can display important temperature effects due to the possible degeneracy of the plasma shells.

Having treated the case of colliding pair plasmas, we will turn to the case of electron/proton plasmas.

We first address in section “Criterion for strong shock” the criterion for strong shock. Then the criterion for collisionless downstream is explained in section “Criterion for collisionless downstream”. Finally, we turn in section “Criterion for collisionless formation” to the criterion for collisionless shock formation necessary to the existence of scattering agents. Section “Merging the three criteria” presents all the criteria together before we explain the case of electron/proton shells in section “Electron/proton shells”, and reach our conclusions.

Criterion for strong shock

The determination of the properties of the shock formed by the collision of two fluids is a typical Riemann problem. The solution of this problem is that a shock is formed regardless of the speed of the collision [see Landau and Lifshitz (2013b) p. 362, or Zel’dovich and Raizer (2002) p. 89]. Yet, in the limit of small collision speed, that is, small Mach number M_0 , the shock density jump reads $r \sim 1 + M_0$ [this is straightforwardly derived from the expression of the jump in terms of M_0 ; see, e.g. Thorne and Blandford (2017), p. 905].

We can therefore set the threshold for efficient acceleration at $M_0 = 1$. The Mach number reads $M_0 = v_0/C_S$ where C_S is the speed of sound, which is proportional to the thermal spread Δv in the shells. We find therefore that the threshold for particle acceleration naturally limits the range of thermal spreads we need to explore. Such a feature will be important to assess the next two criteria in sections “Criterion for collisionless downstream” and “Criterion for collisionless formation”.

Since v_0 can be relativistic, it is convenient to assess $M_0 = 1$ in the reference frame of one shell. In this frame, the density is n_0/γ_0 , and the impact velocity is the relative velocity v_r with,

$$\frac{v_r}{c} = \frac{2\beta_0}{1 + \beta_0^2}, \tag{1}$$

where $\beta_0 = v_0/c$. Then, the equality $M_0 = v_0/C_S = 1$ reads differently according to the regime considered for the shells. The shells can be relativistic or not, and degenerate or not. Let us start with the case of degenerate shells.

- If the shells are initially degenerate, the speed of sound varies with the density. The condition $M_0 = 1$ therefore translates to a condition on n_0 and v_0 . In the non-relativistic regime, the speed of sound reads (Landau and Lifshitz, 2013a),

$$C_S = \frac{V_F}{\sqrt{3}} = \frac{(3\pi^2)^{1/3}}{\sqrt{3}} n_0^{1/3} \frac{\hbar}{m_e}, \tag{2}$$

where V_F is the Fermi velocity and m_e the electron mass. Replacing n_0 by n_0/γ_0 and writing $v_r = C_S$ gives the critical density

beyond which no strong shock forms,

$$n_{0,c} = \frac{8\sqrt{3}}{\pi^2} \left(\frac{m_e c}{\hbar}\right)^3 \frac{\beta_0^3}{(1 + \beta_0^2)^3} \gamma_0, \tag{3}$$

where m_e is the electron mass. This expression is valid as long as $C_S \ll c$. When the density tends to infinity, Eq. (2) has to be amended and the asymptotic value of C_S is $c/\sqrt{3}$. In this regime, the equality $v_r = C_S$ gives therefore a limit value of β_0 beyond which any shock is strong. This critical value is,

$$\beta_0 = \sqrt{3} - \sqrt{2} \sim 0.32. \tag{4}$$

- As long as the shells are dense enough, they are degenerate¹ and the strong shock threshold is given by Eqs. (3) and (4). When the density is such that the Fermi temperature becomes lower than the shells temperature, then the speed of sound is given by,

$$C_S = \begin{cases} \sqrt{\hat{\gamma} \frac{k_B T}{m}} & (k_B T \ll mc^2), \\ \frac{c}{\sqrt{3}} & (k_B T \gg mc^2), \end{cases} \tag{5}$$

where $\hat{\gamma}$ is the adiabatic index of the gas. In this regime, $C_S = v_r$ yields therefore a maximum velocity β_0 beyond which the shock is strong.

The portion of the phase space defined in this section is eventually pictured in Figure 1. For $T_0 = 0$, there cannot be strong shocks to the left of the blue line defined by Eqs. (3) and (4). At low β_0 and for $T_0 = 0$, the frontier is defined by Eq. (3) all the way to $\beta_0 = 0$. Then, for finite temperature T_0 , the frontier turns vertical at a density n_0 defined by $T_F(n_0) = T_0$. In the limit of infinite T_0 , the strong shock threshold is simply a vertical line located at $\beta_0 = \sqrt{3} - \sqrt{2}$ ($\beta_0 \gamma_0 = 0.32$). Beyond this initial velocity, the shock formed must be strong because the speed of sound cannot exceed $c/\sqrt{3}$.

Criterion for collisionless downstream

A plasma is collisionless, or weakly coupled, if it contains more kinetic energy than Coulomb potential energy. If its temperature T is higher than the Fermi temperature T_F (and lower than $m_e c^2$), the weakly coupled regime pertains to,

$$k_B T > q^2 n^{1/3}. \tag{6}$$

When the plasma becomes degenerate, that is, $T < T_F$, the weakly coupled regime pertains to,

$$k_B T_F > q^2 n^{1/3}, \tag{7}$$

where T_F is the Fermi temperature, with $k_B T_F = (3\pi^2 n)^{2/3} \hbar^2 / 2m_e$. Equation (7) gives,

$$n > 6.3 \times 10^{22} \text{ cm}^{-3}. \tag{8}$$

¹See Section 3.

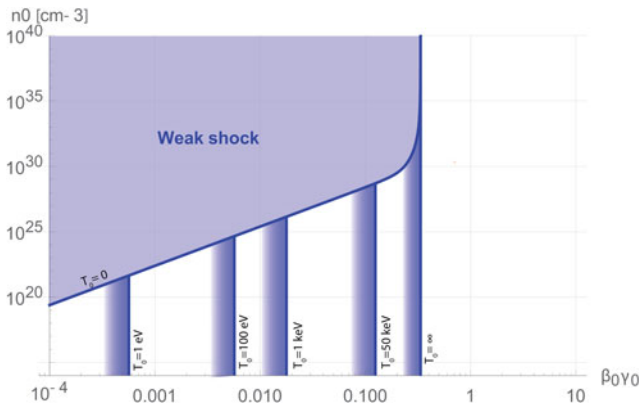


Fig. 1. Strong shock threshold discussed in section “Criterion for strong shock”. For finite comoving temperature T_0 , the limit turns vertical at a density n_0 defined by $T_F(n_0) = T_0$ and no strong shock forms to the left of the corresponding vertical line. In the limit of infinite temperature, the speed of sound tends to $c/\sqrt{3}$ so that all shocks are strong beyond $\beta_0\gamma_0 = 0.32$.

The weakly coupled regime is eventually pictured in Figure 2 by the purple area. When $T < T_F$, density plays the role of the temperature.

Assume, for a start, that the two colliding shells are cold. Upon which conditions on (n_0, v_0) will the downstream be strongly coupled? The downstream of the shock formed by their collision will be at density n and temperature T , both functions of (n_0, v_0) . The non-relativistic² Rankine–Hugoniot relations allow to determine (n, T) in terms of (n_0, v_0) . For a null upstream pressure, they give (Zel’dovich and Raizer, 2002),

$$n = n_0 \frac{\hat{\gamma} + 1}{\hat{\gamma} - 1}, \tag{9}$$

$$k_B T = m_e v_0^2, \tag{10}$$

where $m_e v_0^2$ could be written $2(1/2)m_e v_0^2$, making it clear that the downstream thermal energy comes from the initial kinetic energy of the electrons and the positrons (hence the factor 2). Inverting these relations, we find that if the downstream is degenerate, then it is collisionless for,

$$n_0 < 6.3 \times 10^{22} \left(\frac{\hat{\gamma} - 1}{\hat{\gamma} + 1} \right) \text{ cm}^{-3}. \tag{11}$$

If the downstream is classical, then it is strongly coupled for,

$$n_0 > N^* \left(\frac{\hat{\gamma} - 1}{\hat{\gamma} + 1} \right) \beta_0^6, \tag{12}$$

where,

$$N^* = \left(\frac{m_e c^2}{q^2} \right)^3 = 4.5 \times 10^{37} \text{ cm}^{-3}. \tag{13}$$

The strongly coupled conditions for the downstream translate to the two conditions above on (n_0, v_0) . The corresponding

²We will check at the end of the calculation that relativistic effects do not need to be accounted for.

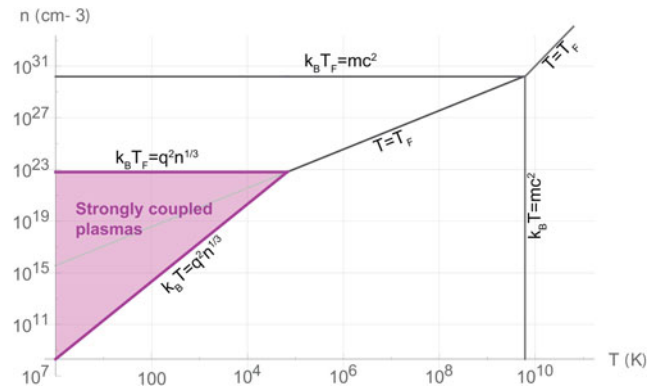


Fig. 2. Plasmas located inside the purple area are strongly coupled, that is, collisional. A shock cannot accelerate particles if either its downstream or its upstream is located within this region.

portion of the phase space parameter (n_0, v_0) is pictured in Figure 3 by the green area. Some frontiers derived in the preceding section have been reproduced. We here check that relativistic effects are irrelevant, as the maximum β_0 involved is ~ 0.004 .

How can a finite T_0 affect the picture? Weakly, simply because criterion 1 studied in section “Criterion for strong shock” imposes a strong shock. Hence, while the equations above are exact in the $T_0 = 0$ limit, they remain valid at first order for a strong shock, and Figure 3 with them.

Criterion for collisionless formation

When the two shells approach each other, their interaction can be of two very different kinds. On the one hand, the binary collision frequency $v_{s,s}$ between particles of two different shells sets the time scale for collisional interaction. On the other hand, if the shells start overlapping, the growth rate δ of the fastest growing mode of the resulting unstable counter-streaming system sets the time scale for collisionless interaction.

If $\delta \ll v_{s,s}$, binary collisions mediate the interaction. The shells encounter is fluid-like, as they do not interpenetrate each other. The outcome of the interaction is also fluid-like, with a shock therefore free of electromagnetic turbulence upstream and downstream.

In the opposite case, when $\delta \gg v_{s,s}$, the interaction is mediated by counter-streaming instabilities. As a result, the overlapping region is quickly filled with an electromagnetic turbulence which blocks the incoming flow and forms the shock (Bret *et al.*, 2013a, 2014). The same electromagnetic turbulence then provides the scattering agents necessary for particle acceleration.

The condition $\delta = v_{s,s}$ is therefore a third criterion for particle acceleration. Let us now compute δ and $v_{s,s}$, before we compare these two quantities.

Largest growth rate

The strong shock criterion established in section “Criterion for strong shock” imposes an initial thermal spread $\Delta v \ll v_0$. We can therefore work here in the cold limit $T_0 = 0$.

The growth rate δ we are interested in is the one of the fastest growing mode in the unstable region. Many unstable modes can grow in this region where the two shells overlap. Two-stream modes grow with a wave vector aligned with the flow (Bohm

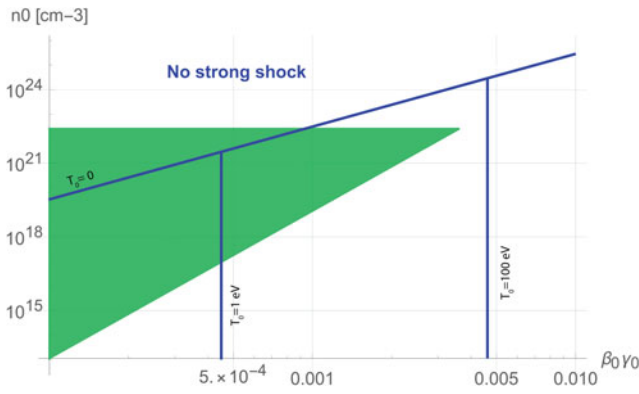


Fig. 3. If the colliding shells parameters lie inside the green triangle, the downstream of the shock will be strongly coupled and the shock unable to accelerate particles. This criterion excludes regions which would be allowed by the strong shock requirement.

and Gross, 1949a, 1949b). Weibel modes grow with a wave vector normal to the flow (Fried, 1959), and oblique modes also grow, with a wave vector oblique to the flow (Faïnberg *et al.*, 1970; Bret *et al.*, 2005, 2006, 2010).

For the present case of two counter-streaming pair beams, the fastest growing modes only depend on γ_0 . They are two-stream like as long as $\gamma_0 < \sqrt{3/2}$ (Bret *et al.*, 2013b). Beyond this, Weibel modes are the fastest growing ones. The quantity δ is eventually given by,

$$\delta = \begin{cases} (1 + \beta_0^2)\sqrt{\frac{\gamma_0}{2}}\omega_p, & \gamma_0 < \sqrt{3/2}, \\ \frac{2\beta_0}{\sqrt{\gamma_0}}\omega_p, & \gamma_0 > \sqrt{3/2}, \end{cases} \quad (14)$$

where $\omega_p^2 = 4\pi n_0 q^2 / m_e$ is the electronic plasma frequency.

Inter-shell binary collision frequency, and comparison with δ

We now compute the binary collision frequency for particles of one shell with particles of the other shell. These particles approach each other at the relative velocity v_r given by Eq. (1). The impact parameter b for close collisions, namely, collisions yielding a deviation of $\pi/2$, reads (Jackson, 1998),

$$b = \max\left(\frac{q^2}{\gamma_r m_e v_r^2}, \frac{\hbar}{\gamma_r m_e v_r}\right), \quad (15)$$

with $\gamma_r = (1 - v_r^2/c^2)^{-1/2}$. The collision frequency $\nu_{s,s}$ then reads,

$$\nu_{s,s} = n_0 v_r \pi b^2. \quad (16)$$

We need now to compare Eqs. (14) and (16). Due to the various expressions involved in several intervals, the corresponding frontier has several breaks. It is pictured by the orange line in Figure 4, which is further commented in the next section.

Merging the three criteria

Figure 4 gathers all the results obtained for pair plasmas. Plasma shells located above the orange line will form a shock through inter-shells binary collisions. Clearly, our three criteria for no

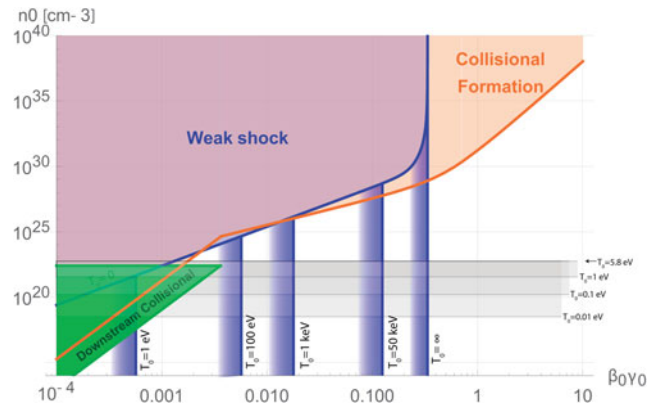


Fig. 4. Representation of the three criteria on a single plot (pair plasmas). The shock formation is mediated by plasma instabilities only below the orange line. The shock formed is strong only below (or to the right of) the blue line. The downstream is collisional inside the green triangle. Regarding the horizontal gray stripes varying with T_0 , see Eqs. (17) and (18) in section “Merging the three criteria”.

particle acceleration largely overlap. However, the only criterion still discriminating for $\beta_0\gamma_0 > 0.32$ (and T_0 large enough, see Eq. 18) is the collisional/collisionless formation one.

The effects of a finite comoving temperature T_0 are readily accounted for. As noted previously, the strong shock requirement imposes $v_0 \gg \Delta v$ so that the growth rate and the inter-shells binary collision frequency used in section “Criterion for collisionless formation”, together with the Rankine–Hugoniot relations used in section “Criterion for strong shock”, remain unchanged. Hence, the green and the blue frontiers are nearly unaffected by $T_0 \neq 0$. Only the criteria for strong shock significantly changes since a finite temperature can result in a sound speed varying with the temperature instead of the density.

Section “Criterion for collisionless downstream” assessed the conditions upon which the downstream is collisional. What about the upstream? Indeed, if our colliding shells (which represent the future upstream) are already collisional, acceleration is also suppressed. The shells are collisional if the parameters (T_0, n_0) lie inside the purple triangle in Figure 2. For a given temperature T_0 , this translates to a collisional “window” for the density n_0 . Therefore, the upstream is collisional if,

$$\begin{aligned} n_0 &\in [n_-(T_0), n_+], \text{ with} \\ n_-(T_0) &= \left(\frac{k_B T_0}{q^2}\right)^3, \text{ and} \\ n_+ &= 6.3 \times 10^{22} \text{ cm}^{-3}. \end{aligned} \quad (17)$$

We reach $n_-(T_0) = n_+$ for,

$$T_0 = \frac{2}{3^{2/3}\pi^{4/3}} \frac{mq^4}{\hbar^2 k_B} = 6.73 \times 10^4 \text{ K} = 5.8 \text{ eV}. \quad (18)$$

Back to Figure 4, this additional criterion defines therefore an horizontal stripe from $n_0 = n_-(T_0)$ to n_+ . The upper limit of the stripe is at n_+ and does not vary with T_0 . The lower limit is at $n_-(T_0)$. It reaches the upper limit for $T_0 = 5.8 \text{ eV}$ so that this criterion for a collisional upstream disappears from the map beyond this temperature. Notably, it turns out that it is perfectly possible to have a collisionless upstream and a collisional downstream, at the same time.

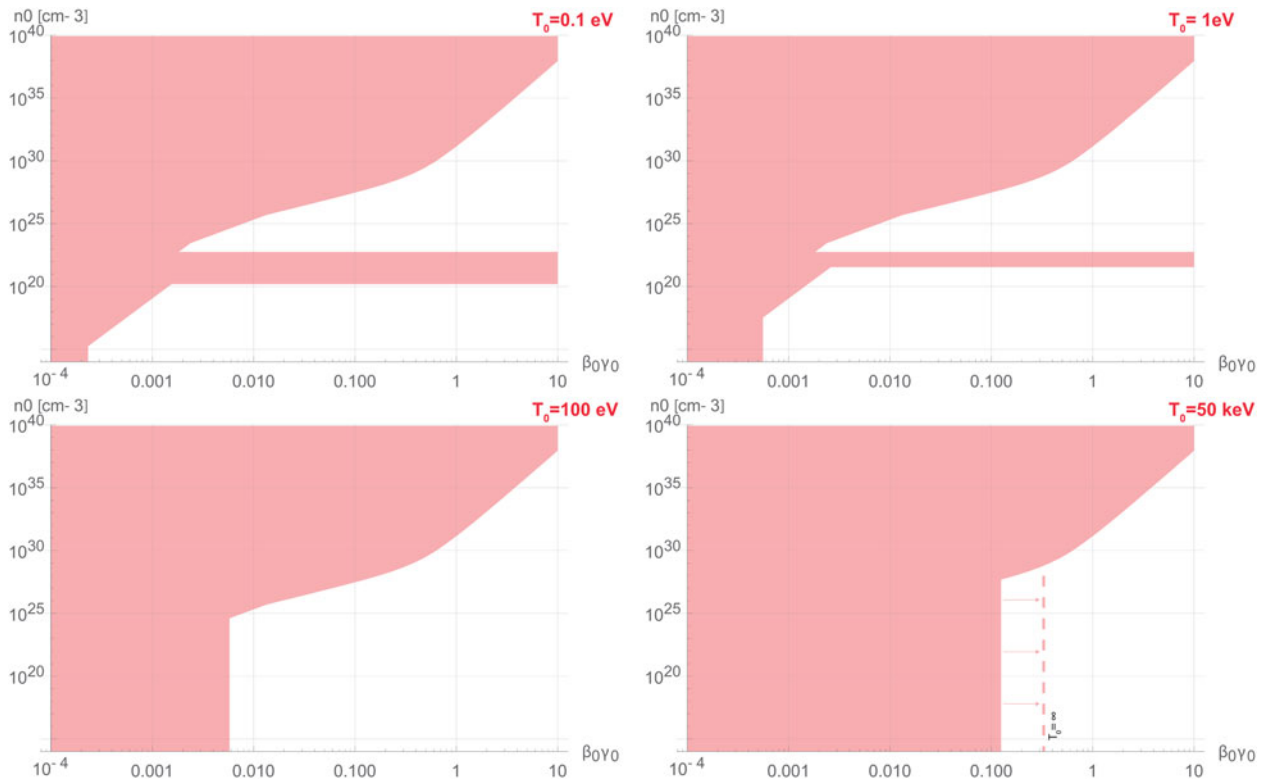


Fig. 5. The shaded area pictures the region of the phase parameter where no particle acceleration can occur for pair plasmas collisions. The four maps are plotted for four different comoving temperatures T_0 . The vertical dashed line on the map for $T_0 = 50$ keV shows the threshold for strong shock in the limit of infinite T_0 .

In order to provide a clearer picture of the portion of the $(\beta_0\gamma_0, n_0)$ phase space allowing particle acceleration, Figure 5 represents all the forbidden zones with a unique shading, and for four values of the comoving temperature T_0 . At low T_0 , the resulting map is highly non-trivial as the three criteria do not fully overlap. At high T_0 , only the strong shock criteria (at low densities) and the collisionless formation criteria shape the map.

Electron/proton shells

The case of electron/proton (e/p) shells can be nearly straightforwardly adapted from the pair shells treated previously.

The strong shock requirements for e/p shells are derived replacing the electron mass by the proton mass m_p in section “Criterion for strong shock”. The reason for this is that the sound speed is formally given by $C_s^2 = \partial P / \partial \rho$, where the density ρ now comes from the protons.

The strongly coupling criteria is also retrieved replacing the electron mass m_e by the proton mass m_p in section “Criterion for collisionless downstream”.

Regarding the criteria for collisionless formation of section “Criterion for collisionless formation”, we need to now focus on the protons, since they control the dynamics of the shock formation. The inter-shell collision frequency $v_{s,s}$ is obtained replacing the electron mass m_e by the proton mass m_p in Eqs. (15) and (16). The maximum growth rate needs slightly more adjustments, for two reasons.

(1) In pair plasmas, the dominant instability grows and then, the shock formation starts (Bret *et al.*, 2014; Dieckmann and Bret, 2017; Dieckmann and Bret, 2018). The process is one stage.

In e/p plasmas, the electrons turn unstable first. The related dominant instability grows and saturates. At that stage, owing to the large mass ratio involved, the protons are still counter-streaming over the bath of randomized electrons. Then they turn unstable and form the shock. The process is therefore two stages (Stockem Novo *et al.*, 2015).

(2) From the point above, we infer that the growth rate δ we need to compare with the inter-shell collision frequency is the one of the counter streaming protons over the bath of electrons.

Evaluating δ here is both different and simpler. Different because the unstable system under scrutiny is different. Simpler because we only need to focus on the non-relativistic regime. Indeed, as will be checked later, the equality $\delta = v_{s,s}$ translates to physically meaningful proton densities (say $n_0 < 10^{40} \text{ cm}^{-3}$) only in the non-relativistic regime.

We therefore need to find the maximum growth rate of the unstable system formed by two counter-streaming cold proton beams at $\pm v_0$, over a bath of electrons. The derivation of the growth rate δ can be performed noting that in the limit of small velocities, the background electrons are cold since their thermal energy comes from their initial kinetic energy. For such a system, the fastest growing instability is the two-stream instability (Bret *et al.*, 2008, 2010), with a dispersion equation given by (Ichimaru, 1973),

$$\frac{2}{x^2} + \frac{R}{(Z-x)^2} + \frac{R}{(x+Z)^2} = 1, \tag{19}$$

where $x = \omega/\omega_p$, $Z = kv_0/\omega_p$ and $R = m_e/m_p$. Note that ω_p is still the electronic plasma frequency. Since $R \ll 1$, the roots of this

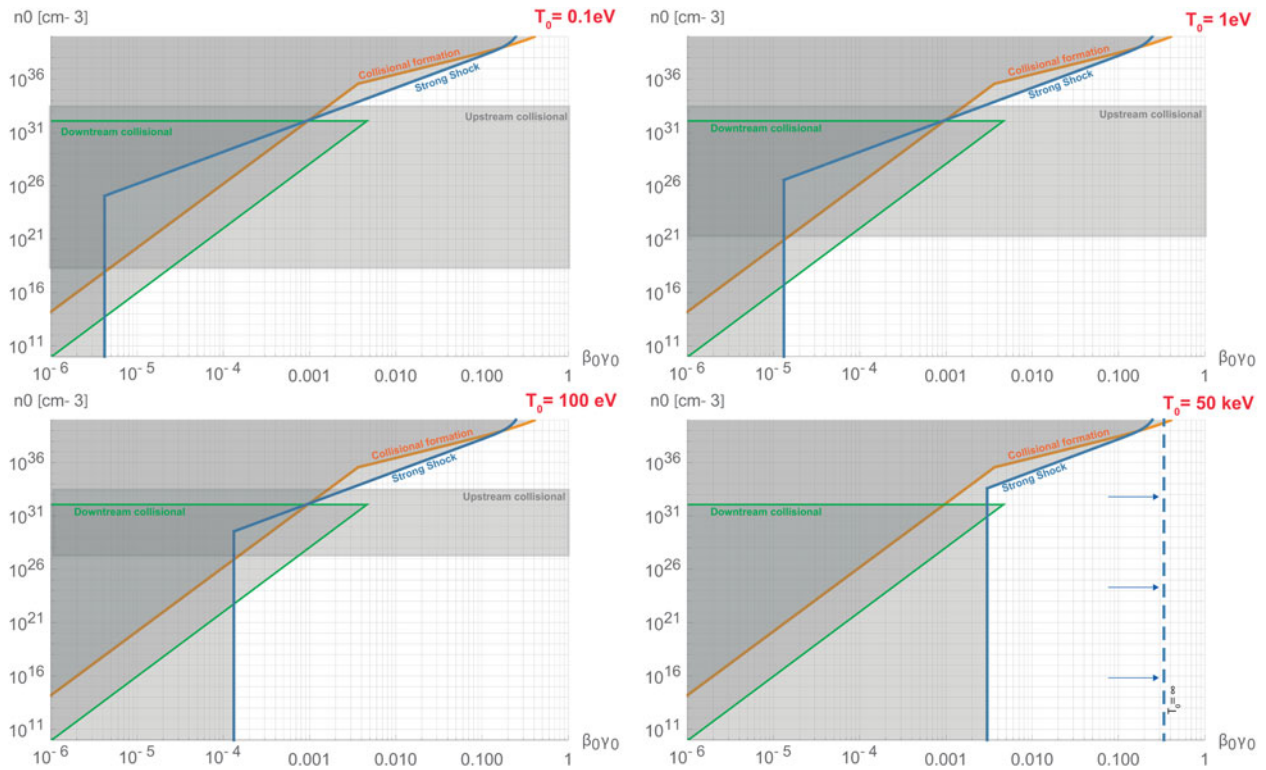


Fig. 6. Region of the $(\beta_0\gamma_0, n_0)$ phase space allowing particle acceleration for an e/p shock, for four comoving temperatures T_0 . The shaded areas forbid acceleration. The horizontal stripe forbidding acceleration because the upstream would be collisional, vanishes for $T_0 > 10.6$ keV. The vertical dashed line on the map for $T_0 = 50$ keV shows the threshold for strong shock in the limit of infinite T_0 .

equation have to be close to $x = \pm\sqrt{2}$. Hence, in terms of Z , they will be found near $Z = \pm\sqrt{2}$, for the denominator of the terms $\propto R$ has to be small since their numerator is small. Focusing on the solution near $Z = +\sqrt{2}$, we can drop the term $\propto (x + Z)^{-2}$ and set $x = \sqrt{2} + \epsilon$. A Taylor expansion in ϵ gives,

$$\delta = \mathfrak{S}(\epsilon) = \frac{\sqrt{3}}{27^{1/6}} R^{1/3} \omega_p. \tag{20}$$

Assessing $\delta = v_{s,s}$ is then straightforward from Eqs. (15, 16, 20).

Finally, comoving temperature effects are similar to the pair case. The strong shock limit is obtained from section ‘‘Criterion for strong shock’’ replacing m_e by m_p , and the upstream is collisional for $n_0 \in [n_-(T_0), n_+]$, where $n_-(T_0)$ is given by Eq. (17) and $n_+ = 3.88 \times 10^{32} \text{ cm}^{-3}$. Here, $n_-(T_0) = n_+$ is reached for $T_0 = 10.6$ keV. Beyond this temperature, the colliding e/p plasmas are collisionless regardless of their density n_0 .

Figure 6 pictures the three criteria for e/p plasmas and four comoving temperatures. The plot for $T_0 = 50$ keV also features the asymptotic position of the strong shock threshold in the limit $T_0 = \infty$. It is found equal to the pair case since it is the result of the speed of sound being limited by $c/\sqrt{3}$ in both settings.

Conclusion

We considered the shock formed by the encounter of two identical pair plasma shells characterized by the parameters (n_0, T_0, γ_0) . We assessed three criteria for particle acceleration, namely (1) that the shock must be strong, (2) that neither the downstream nor the upstream can be collisional, and (3) that the shock formation

must have been mediated by plasma instabilities which seed the scattering agents essential for particle acceleration.

Figures 4–6 summarize how these criteria translate to the parameters (n_0, T_0, γ_0) for pair and e/p plasmas. The resulting maps are non-trivial as the three criteria do not overlap.

Future works could account for various additional effects. An external magnetic field would modify the Rankine–Hugoniot relations and the growth rate calculations, for example. Also, astrophysical settings often involve radiative shocks (Bouquet *et al.*, 2000, 2004) in which radiation pressure and energy must be accounted for in the Rankine–Hugoniot budget. As a consequence, the allowed regions for particle acceleration would also be modified.

Author ORCIDs. Antoine Bret 0000-0003-2030-0046.

Acknowledgments. A.B. acknowledges support by grants ENE2016-75703-R from the Spanish Ministerio de Educación and SBPLY/17/180501/000264 from the Junta de Comunidades de Castilla-La Mancha. A.P. acknowledges support by the European Union Seventh Framework Program (FP7/2007-2013) under grant agreement no. 618499, and support from NASA under grant no. NNX12AO83G. A.B. thanks Gustavo Wouchuk, Roberto Piriz for fruitful discussions.

References

Bale SD, Mozer FS and Horbury TS (2003) Density-transition scale at quasi-perpendicular collisionless shocks. *Physical Review Letters* **91**, 265004.
 Blandford R and Eichler D (1987) Particle acceleration at astrophysical shocks: a theory of cosmic ray origin. *Physics Reports* **154**, 1.
 Blandford R and Ostriker J (1978) Particle acceleration by astrophysical shocks. *Astrophysical Journal* **221**, L29.

- Bohm D and Gross EP** (1949a) Theory of plasma oscillations. a. Origin of medium-like behavior. *The Physical Review* **75**, 1851.
- Bohm D and Gross EP** (1949b) Theory of plasma oscillations. b. Excitation and damping of oscillations. *The Physical Review* **75**, 1864.
- Bouquet S, Romain T and Chieze JP** (2000) Analytical study and structure of a stationary radiative shock. *The Astrophysical Journal Supplement Series* **127**, 245–252.
- Bouquet S, Stéhlé C, Koenig M, Chièze J-P, Benuzzi-Mounaix A, Batani D, Leygnac S, Fleury X, Merdji H, Michaut C, Thais F, Grandjouan N, Hall T, Henry E, Malka V and Lafon J-PJ** (2004) Observation of laser driven supercritical radiative shock precursors. *Physical Review Letters* **92**, 225001.
- Bret A, Firpo M-C and Deutsch C** (2005) Bridging the gap between two stream and filamentation instabilities. *Laser and Particle Beams* **23**, 375–383.
- Bret A, Firpo M-C and Deutsch C** (2006) Between two stream and filamentation instabilities: temperature and collisions effects. *Laser and Particle Beams* **24**, 27–33.
- Bret A, Gremillet L, Bénisti D and Lefebvre E** (2008) Exact relativistic kinetic theory of an electron-beam-plasma system: hierarchy of the competing modes in the system-parameter space. *Physical Review Letters* **100**, 205008.
- Bret A, Gremillet L and Dieckmann ME** (2010) Multidimensional electron beam-plasma instabilities in the relativistic regime. *Physics of Plasmas* **17**, 120501.
- Bret A, Stockem A, Fiúza F, Pérez Álvaro E, Ruyer C, Narayan R and Silva LO** (2013a) The formation of a collisionless shock. *Laser and Particle Beams* **31**, 487–491.
- Bret A, Stockem A, Fiúza F, Ruyer C, Gremillet L, Narayan R and Silva LO** (2013b) Collisionless shock formation, spontaneous electromagnetic fluctuations, and streaming instabilities. *Physics of Plasmas* **20**, 042102.
- Bret A, Stockem A, Narayan R and Silva LO** (2014) Collisionless Weibel shocks: full formation mechanism and timing. *Physics of Plasmas* **21**, 072301.
- Dieckmann ME** (2005) Particle simulation of an ultrarelativistic two-stream instability. *Physical Review Letters* **94**, 155001.
- Dieckmann ME and Bret A** (2017) Simulation study of the formation of a non-relativistic pair shock. *Journal of Plasma Physics* **83**, 905830104.
- Dieckmann ME and Bret A** (2018) Electrostatic and magnetic instabilities in the transition layer of a collisionless weakly relativistic pair shock. *Monthly Notices of the Royal Astronomical Society* **473**, 198–209.
- Fainberg YB, Shapiro VD and Shevchenko V** (1970) Nonlinear theory of interaction between a monochromatic beam of relativistic electrons and a plasma. *Journal of Experimental and Theoretical Physics* **30**, 528.
- Fried BD** (1959) Mechanism for instability of transverse plasma waves. *Physics of Fluids* **2**, 337.
- Ichimaru S** (1973) *Basic Principles of Plasma Physics*. Reading, MA: W. A. Benjamin, Inc.
- Jackson J** (1998) *Classical Electrodynamics*. Hoboken, NJ: Wiley.
- Kirk JG and Duffy P** (1999) Particle acceleration and relativistic shocks. *Journal of Physics G: Nuclear and Particle Physics* **25**, R163.
- Landau L and Lifshitz E** (2013a) *Course of Theoretical Physics, Statistical Physics*. Number v. 5. Amsterdam, Netherlands: Elsevier Science.
- Landau L and Lifshitz E** (2013b) *Fluid Mechanics*. Number v. 6. Amsterdam, Netherlands: Elsevier Science.
- Lemoine M, Pelletier G, Gremillet L and Plotnikov I** (2014) A fast current-driven instability in relativistic collisionless shocks. *EPL (Europhysics Letters)* **106**, 55001.
- Marcowith A, Bret A, Bykov A, Dieckmann ME, Drury L, Lembège B, Lemoine M, Morlino G, Murphy G, Pelletier G, Plotnikov I, Reville B, Riquelme M, Sironi L and Stockem Novo A** (2016) The microphysics of collisionless shock waves. *Reports on Progress in Physics* **79**, 046901.
- Nakar E, Bret A and Milosavljević M** (2011) Two-stream-like instability in dilute hot relativistic beams and astrophysical relativistic shocks. *Astrophysical Journal* **738**, 93.
- Niemiec J, Pohl M, Bret A and Wieland V** (2012) Nonrelativistic parallel shocks in unmagnetized and weakly magnetized plasmas. *Astrophysical Journal* **759**, 73.
- Ruyer C, Gremillet L, Bonnaud G and Riconda C** (2017) A self-consistent analytical model for the upstream magnetic-field and ion-beam properties in Weibel-mediated collisionless shocks. *Physics of Plasmas* **24**, 041409.
- Sagdeev RZ** (1966) Cooperative phenomena and shock waves in collisionless plasmas. *Reviews of Plasma Physics* **4**, 23.
- Schwartz SJ, Henley E, Mitchell J and Krasnoselskikh V** (2011) Electron temperature gradient scale at collisionless shocks. *Physical Review Letters* **107**, 215002.
- Stockem Novo A, Bret A, Fonseca RA and Silva LO** (2015) Shock formation in electron-ion plasmas: mechanism and timing. *Astrophysical Journal Letters* **803**, L29.
- Thorne K and Blandford R** (2017) *Modern Classical Physics: Optics, Fluids, Plasmas, Elasticity, Relativity, and Statistical Physics*. Princeton, NJ: Princeton University Press.
- Yuan D, Li Y, Liu M, Zhong J, Zhu B, Li Y, Wei H, Han B, Pei X, Zhao J, Li F, Zhang Z, Liang G, Wang F, Weng S, Li Y, Jiang S, Du K, Ding Y, Zhu B, Zhu J, Zhao G and Zhang J** (2017) Formation and evolution of a pair of collisionless shocks in counter-streaming flows. *Scientific Reports* **7**, 42915.
- Zel'dovich I and Raizer Y** (2002) *Physics of Shock Waves and High-Temperature Hydrodynamic Phenomena*. Dover Books on Physics. Mineola, NY: Dover Publications.